AUTOMATED VISUALIZATION OF TEETH IN 3D CT Data

Sh. Keyhaninejad [*1], R. A. Zoroofi [*2], S. K. Setarehdan [*3], Gh. Shirani[**], M. Jahangiri[***]

*Control and Intelligent Processing Canter of Excellence, School of Electrical and Computer Engineering Faculty of Engineering, University of Tehran, Tehran, IRAN.

**Oral & Maxillofacial Surgery Department, Faculty of Dentistry Medical Science of Tehran University,Tehran, IRAN

***Research Associate Imperial College of London Electrical and Electronis Department

e-mail:shiva_keyhani@yahoo.com[*1], zoroofi@ut.ac.ir[*2], ksetareh@ut.ac.ir[*3]

Abstract-**Automatic quantification and volumetric visualization of teeth is of clinical importance for various computer assisted procedures such as dental implant, orthodontic planning, face, jaw and cosmetic surgeries. In this paper we propose an algorithm for automatic quantification and visualization of teeth in 3D CT data set. This algorithm consists of three main steps. In the first step a classification algorithm that was proposed by the authors is applied to 3D CT data. The classification is based on a geometric type of active contours, i.e, level sets together with panoramic re-sampling of the data set. Next, a metal artifact reduction (MAR) algorithm is applied to the slices that are severely damaged by this effect. The MAR algorithm is based on the low pass Butterworth filtering which is applied in the frequency domain. In the last step a surface rendering algorithm known as Marching Cube is applied to the classified slices for the purpose of volumetric visualization.**

The proposed algorithm was applied to 10 different CT datasets. The objective and subjective tests of the proposed algorithm show promising and applicable results

Keywords **Active contour, Level sets, Panoramic re-sampling, Metal artifact reduction, Marching cube**

I. INTRODUCTION

Nowadays, different medical imaging techniques are the indispensable part of medicine for acquiring both functional and anatomical information from the body. For years, X-ray transmission-based radiographs were the basis of medical imaging. However, with the advent of computerized transverse axial scanning (computed tomography, or CT) the main limitation of data acquired from radiographs in which they are two-dimensional projection of some complex intrinsically three-dimensional anatomy, was resolved. In fact, the tomography techniques not only facilitated access to the internal morphology of soft tissue and skeletal structures but also using the digital visualization procedures and algorithms access to the 3 dimensional views of intrinsically three –dimensional anatomy was enabled. The volumetric data is the main source of different medical applications and clinical studies ranging from 3D visualization to quantitative studies.

Teeth are one of the most important anatomical structures in the facial beauty and healthiness that inspire a wide range of clinical studies and applications. Automatic quantification and 3-D visualization of teeth are of clinical importance for various computer-assisted procedures such as dental implant, orthodontic planning, face, jaw, and cosmetic surgeries. For diagnosing dental syndromes, investigation of filled and decayed teeth, precise geometrical measurements, segmentation procedures and 3-D visualization are of greatly medical importance. In this work, we proposed an algorithm for the 3-D visualization of dental structures. The proposed algorithm can be utilized in various medical applications such as orthodontic planning, face and jaw surgeries in which the spatial and relative positions are of important factors. Furthermore, the automatic segmentation algorithm that is proposed by the authors can be used in forensic investigations such as human identification. The proposed algorithm is according to the following three steps:

1) Classification
2) Metal Artifact Reduction
3) Surface rendering

The classification step is based on the work that was done by the authors in [1]. In [1] after obtaining the head mask, bony tissues are classified from non-bony tissues by a level set technique [2],[3],[4],[5]. Next, the teeth are segmented from other bony tissues by imposing anatomical constraint with intensity of associated with intensity of teeth in the jaws. The proposed method [1] is followed by estimating the arc of the upper and lower jaws and panoramic re-sampling of the data set. Separation of upper and lower jaws and initial segmentation of teeth are performed by employing the horizontal and vertical projections of the panoramic data set, respectively. In this case, an initial mask for each tooth is obtained. We then relocated the initial mask on the original data set and apply the level set algorithm to refine each initial boundary to the final tooth contour. More detailed description of this approach is given in section 2-A. The second step of the proposed algorithm is to reduce the effect of metal artifact in the CT slice images which are posed to this undesirable effect. Metal artifacts are a major problem in computed tomography. They are caused by the presence of strongly attributing objects such as dental fillings, prosthetic devices, and surgical clips. For addressing the problem, the slices with metal artifact are detected by their high intensity value. Having selected the slices which are damaged by metal artifact, a Butterworth low pass filtering is applied in the Fourier domain of these slices. More detailed description of this step is given in section 2-B.

For surface rendering of segmented teeth and jaws, the well-known Marching cube algorithm that creates triangle models of constant density surfaces from 3D medical data, was used[6]. Furthermore, (for visualization purposes) in order to distinguish the gingival regions from the teeth regions a color scheme is designed to differ these two regions. More detailed description of this step is given in section 2-C.

In section 2 the above mentioned steps are described in detail. In section 3 some of the experimental results of the proposed algorithm are depicted and discussed. Section 4 the drawn conclusions are given.

II. METHODOLOGY

To describe the proposed scheme, we first recall the basic setting for automated segmentation algorithm, which

presented in [1]. In previous work, the level set algorithm was used for teeth segmentation.

Level set method is a numerical technique, which follows the propagation of contours, surfaces and is particularly useful for segmentation. Rather than tracking the movement of a given closed contour Γ, and a speed function, F, that gives the speed of Γ in its normal direction $\vec{n}$ according to the evolution equation, the signed distance function ϕ is considered. Then, by the chain rule, an evolution equation for the interface is produced [4]:

$$\phi_t + F|\nabla\phi| = 0 \qquad (1)$$

A. Classification

For tooth segmentation, we use multi-step segmentation algorithms based on level set [2],[3],[4].The proposed techniques are explained as follow:

1) *Segmentation of Bony Tissues from other Tissues*

We classified bony tissues from non-bony tissues by applying the level set technique with considering some image forces to stop evolving contour on the boundary of the desired objects. In this case, the Euler equation is written as:

$$\frac{\nabla\phi}{\nabla t} = C(x)(\kappa + V_0)|\nabla\phi| + \nabla C.\nabla\phi + \frac{V_0}{2}(x.\nabla C)|\nabla\phi| \qquad (2)$$

where ϕ is the level set distance function; *k* is the curvature; V_0 is a constant force that imposes to the contour; and $C(x)$ is defined based on the blurred version of the original image.

2) *Segmentation of Teeth from other Bony Tissues*

For, separating teeth from other bony tissues that are of similar intensities, another group of methods, which are based on region characteristics such as Active contour without edge [7], is used.

$$E(C_1, C_2, \phi) = \mu Length(C) + v.Area(Inside(C)) + \lambda_1 \int_{inside(C)} |u_0(x,y) - C_1|^2 dxdy + \lambda_2 \int_{outside(C)} |u_0(x,y) - C_2|^2 dxdy \qquad (3)$$

where, $u_0(x, y)$ is the original image; C_1 and C_2 are associated with the average of intensity inside and outside of the contour, respectively; λ_1 and λ_2 controls the force on the contour; and $\mu \geq 0, v \geq 0, \lambda_1, \lambda_2 \geq 0$.Using Level Set method, we can solve the equation (3), with an initial contour as follows:

$$\frac{\partial\phi}{\partial t} = \delta(\phi)\left[\mu\, div\left(\frac{\nabla\phi}{|\nabla\phi|}\right) - v - \lambda_1(u_0 - C_1)^2 + \lambda_2(u_0 - C_2)^2\right] \qquad (4)$$

where, u_0 is the original image and $\delta(\phi)$ is the Dirac delta function that approximated as follows:

$$H(z) = \begin{cases} 1 & if \quad z > \varepsilon \\ 0 & if \quad z < -\varepsilon \\ \frac{1}{2}\left[1 + \frac{z}{\varepsilon} + \frac{1}{\pi}\sin\left(\frac{\pi z}{\varepsilon}\right)\right] & if \quad |z| \leq \varepsilon \end{cases} \qquad (5)$$

where, *H* (z) is an approximated unit step function; $\delta(\phi)$ is the derivative of *H* (z); and ε is of positive value that is close to zero. Equation (4) was applied to the resultant dataset obtained in part (1). In this case, teeth are separated from other bony tissues.

3) *Panoramic Re-sampling of the Dataset*

It is known that the shape, size and location of each tooth in different axial slices of the acquired CT images might be quite different. In addition, shapes of teeth are different from each other. After finding the slice, which separates the slices of two jaws, the arcs of the both jaws are founded separately in the slices with largest teeth tissues. The orthogonal lines corresponding to the arc were then calculated. The volumetric CT data was then re-sampled with respect to these orthogonal lines. We performed the panoramic image of the data set by coronal projection of the re-sampled data. The initial separation between upper and lower jaws in panoramic image was made by calculating the lowest intensity in the horizontal projection:

$$H(i) = \sum_{j=1}^{n} f(i, j) \qquad (6)$$

where *f(i,j)* is the panoramic image [8]. The initial line was then refined by using a conventional snake. After separating the upper and lower teeth, the initial boundary of each tooth was performed by calculating the valleys of the vertical projection, *V(j)* associated with the panoramic image,

$$V(j) = \sum_{i=1}^{m} f(i, j) \qquad (7)$$

4) *Final Segmentation of Teeth in Volumetric CT Data*

In this section, the initial boundaries performed in (3) are employed to estimate the final contour of each tooth. In this regard, the estimated vertical lines in the panoramic images that separate teeth from each other are equivalent to the volume of interest (VOI) in the original CT data. Hence, the VOI associated with each tooth was relocated in the original CT volume. We applied the algorithm of part (2) to the relocated initial contours of the teeth in the data set and refined contours of teeth were performed.

B. Metal Artifact Reduction:

Referring to the achieved results the metal artifacts are severely damaged image quality and render the image unusable for diagnosis. For addressing this problem, by using the result obtained in part (2) the slices with metal artifacts are detected with their high intensity value. The Butterworth low pass filtering is applied in the Fourier domain of these slices as follows:

$$H(u,v) = \frac{1}{1 + [D(u,v)/D_0]^{2n}} \qquad (8)$$

Where in our work the order of the filter, n=5 and cutoff frequency, D_0 equal to 2% of the padded image width. With this approach, the metal artifact is reduced.

C. Surface Rendering

For surface rendering of segmented teeth and jaws, we used an algorithm, called Marching cube that creates triangle models of constant density surfaces from 3D medical data [6]. Using a divide-and-conquer approach to generate inter-slice connectivity, a case table that defines triangle topology is

created. In this algorithm, we first specify a threshold value. For this value, some voxels will be entirely inside or outside the corresponding iso-surface and some voxels will be intersected by the iso-surface. In the first pass of the algorithm, the voxels that are intersected by the threshold value are identified. In the second pass these voxels are examined and a set of one or more polygons is produced, which are then output for rendering

Marching Cubes is an algorithm for rendering iso-surfaces in volumetric data. The basic notion is that we can define a voxel (cube) by the pixel values at the eight corners of the cube. If one or more pixels of a cube have values less than the user-specified iso-value, and one or more have values greater than this value, we know the voxel must contribute some component of the iso-surface. By determining which edges of the cube are intersected by the iso-surface, we can create triangular patches which divide the cube between regions within the iso-surface and regions outside. By connecting the patches from all cubes on the iso-surface boundary, we get a surface representation.

The teeth that were segmented according to the proposed algorithm in section 2-A, are visualized via the mentioned marching cube technique. Furthermore, in order to discriminate the teeth from the non-bony parts (gingiva), the complement of segmented dental regions are considered as the non-bony parts. These non-bony parts are visualized in a different color (red) as well.

III. RESULTS

The proposed algorithm was applied to 10 different CT multi-slice data sets that were taken from 10 different patients. The test data set were of different dental structures, shapes, sizes and amount of metal artifact. The algorithm was designed via Matlab 7.1 software and VTK tool kit, using visual C++ compiler. The experiments were performed on a Pentium IV

(3.00 GHz, 1GB memory) personal computer (PC).The run-time of this algorithm is between 15 to 20 minutes. It depends on the quality and the number of slices. Furthermore, the user of the proposed package can select a tooth or a group of teeth and visualize them individually or in a group.

We utilized the ROC curve for segmentation method evaluation. A Receiver Operating Characteristic (ROC) curve allows us to explore the relationship between the sensitivity (TPR) and false-positive rate (1-specificity) of our proposed method with other methods of segmentation. For each data set, a dentist performed manual segmentation of teeth.

$$TPR = \frac{TP}{TP + FN} \qquad (9)$$

$$FPR = \frac{FP}{FP + TN}$$

These values were corresponding to three types of tissues.

† TP pixels: correctly segmented dental segments,

† FP pixels: non-dental segments recognized as dental segments due to the failure of the method

† FN pixels: missed dental segments.

The comparison of the different parts of the classification with thresholding is given in Fig. 1 and Fig. 2 respectively.

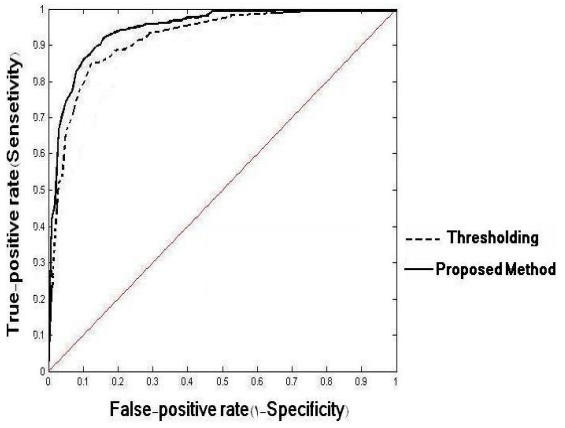

Fig. 1. The ROC curves of the first part of the proposed method and Thresholding

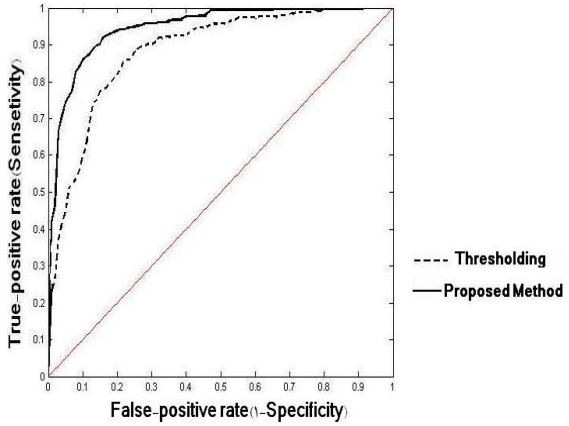

Fig. 2. The ROC curves of the second part of the proposed method and thresholding

The results of the proposed method are compared with two segmentation methods such as watershed and thresholding methods (Fig. 3).

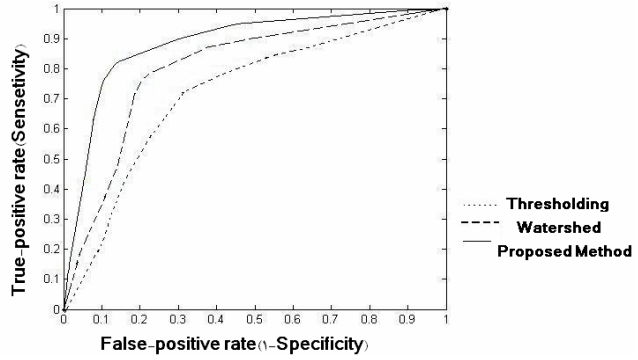

Fig. 3. The ROC curves of the proposed method, watershed & Thresholding

Regarding the Roc curves in Fig. 1, methods, proposed method and thresholding have good results for segmenting bony tissues from other tissues. But in Fig. 2 is shown that our method has better results in segmenting teeth from other

bony tissues. The ROC curves in Fig. 3 shows the weakness of the other methods against our method.
Fig 4.a shows the 3-D visualization of different parts of the face. Fig 4.b is the 3-D visualization of bony structures. It can be seen that due to metal artifact, some parts of this figure are damaged. Fig 5.a shows the 3-D visualization of the whole dental structures. It can be seen that the gingival part are rendered as red. However, metal artifact damages some parts of this figure. Figure 5.b shows the 3-D visualization after the proposed metal artifact reduction algorithm. Figure 5.c depict the visualization of an individual tooth before and after the MAR algorithm. The improvements are clear.

IV. Conclusion

We have proposed an automatic method for segmentation and 3-D visualization of teeth in volumetric CT data. The proposed techniques require no user interaction throughout the procedures. The classification was based on the level set algorithm together with panoramic re-sampling of the data set in the coronal view. Furthermore, a novel metal artifact algorithm for improving the efficiency of the classification was proposed. The 3-D visualization was based on a surface rendering algorithm known as marching cube algorithm. Having applied this method on 10 different volumetric CT data, promising results were obtained. Performing the proposed method in computed assisted surgical planning and dental biometric is our future work.

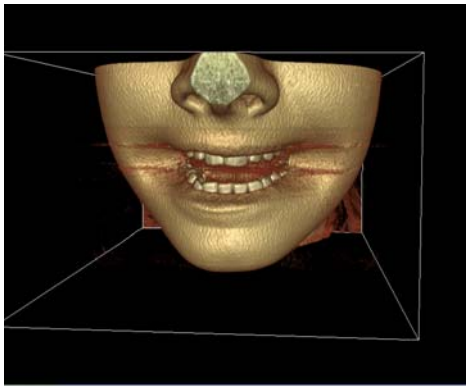

(a)

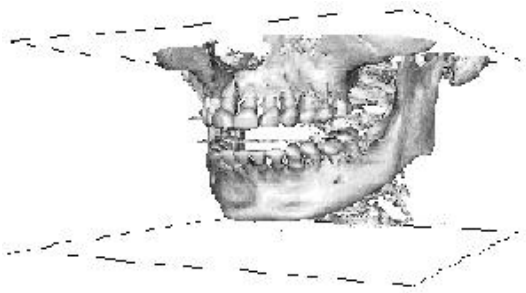

(b)

Fig 4: a) 3-D visualization of different parts of the face. b) 3-D visualization of the bony structures of the face including mandible and maxilla. The effect of metal artifact is clear

(a)

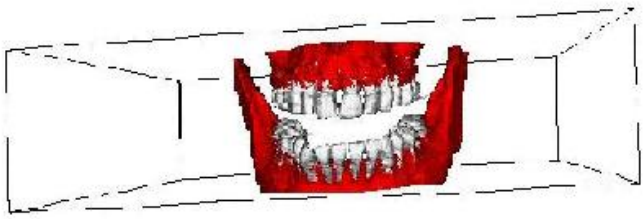

(b)

(c)

Fig 5: a) The 3-D visualization of dental structures. The gingival parts are rendered as red. The damage of metal artifact is clear. b) The 3-D visualization of dental structures after applying the MAR algorithm. c) The 3-D visualization of an individual tooth that is corrupted by metal artifact (left), visualization of an individual tooth after MAR algorithm(right)

References

[1] Sh. Keyhaninejad, R. A. Zoroofi, S. K. Setarehdan, Gh. Shirani**, "**Automated Segmentation of Teeth in Multislice CT Images," In Proc. 3th International Conference On Visual Information Engineering (VIE2006), September 26 -28, India, 2006.

[2] R. Malladi, J.A. Sethian, B. C. Vemuri, "Shape modeling with Front Propagation: A Level Set Approach," IEEE Trans. Pattern Anal. Mach. Intell, Vol. 17, No.2, pp.158-175, 1995.

[3] W. J. Nissen, M. A. Veirgever, "Geodesic Deformable Models for Medical Image Analysis," IEEE Trans. Med. Imag, Vol. 17, No. 4, pp.634-641, 1998.

[4] S. Osher, J. Sethian, "Fronts Propagating with curvature-dependant Algorithms based on Haminlton-Jacobi formulation," J. Comput. Phys., Vol. 79, pp. 12-49, 1988.

[5] J.S. Suri, K. Liu, S. Singh, S. N. Laxminarayan, X. Zeng, L. Reden, "Shape Recovery Algorithms Using Level Sets in 2-D/3-D Medical Imagery: A State-of-the-Art Review," IEEE Trans. Inf Technol Biomed, Vol. 6, No.1, pp. 8-28, 2002.

[6] W. Lorensen, H. Cline, "Marching Cubes: A High Resolution 3D Surface Construction Algorithm," ACM Computer Graphics, Vol. 21, No. 4, pp. 163-170, 1987.

[7] T. F. Chan, "Active Contours Without Edges," IEEE Trans. Image Process, Vol.10, No. 2, pp. 266-277, 2001.

[8] O. Nomir, M.Abdel–Motaleb, "A system for human identification from X-ray dental radiographs," Pattern Recognition, Vol. 38, No. 8, pp. 1295-1305. 2005.